

## Demonstration of a Precision Data Reduction Technique for Navigation of Interplanetary Spacecraft

S. Bhaskaran, S. W. Thurman, and V. M. Pollmeier

Jet Propulsion Laboratory  
California Institute of Technology  
Pasadena, California

Traditional navigation of interplanetary spacecraft involves the fitting of Doppler, range, and ADOR tracking data to a mathematical model of the trajectory. The models used to describe the spacecraft motion and error sources affecting the data were necessarily limited by the time and cost of running the programs on the computers available at the time. With the advent of inexpensive, high-speed computer workstations, these models can be refined to improve the accuracy of the estimated solutions. A demonstration of a more sophisticated data reduction technique, dubbed the "enhanced" filter, has been performed using data from the Galileo spacecraft. Using cases from Galileo's second Earth encounter and a flyby of the asteroid Ida, the enhanced filter is shown to substantially improve the accuracy of the orbit determination solution using Doppler and range data only. The accuracies are comparable to solutions using a standard filter model employing Doppler, range and ADOR data.

### INTRODUCTION

In most interplanetary missions, navigation is accomplished through the use of radio tracking data **acquired** by ground stations from the spacecraft. Radio metric observations, or "data types," used for navigation include two-way Doppler and ranging data derived from a coherent station-spacecraft link, and data types obtained through simultaneous tracking of the spacecraft from two different stations, such as differential Doppler and delta-Differential One-way Range (ADOR). The ADOR data type involves observations of a natural radio source as well as the spacecraft. The navigational accuracy that can be obtained from radio tracking data is principal] y determined by the data types employed and their **precision**, and the **accuracy** with which the spacecraft dynamics and the tracking data can be modeled mathematically in the data reduction process.

Until the development of high-speed computer workstations, the sophistication of the data reduction algorithms used in mission operations was limited primarily by the time and cost associated with the computations, rather than any fundamental inability to accurately model the navigation problem. The onset of relatively cheap, but powerful computing platforms and graphics oriented software tools now makes it possible to develop and employ new data processing schemes to take advantage of the capabilities of these machines. Several navigation demonstrations of more sophisticated data reduction schemes have been conducted recently [Ref. 1, 2], using tracking data obtained from the **Ulysses** and Galileo spacecraft. These demonstrations, which focused on the use of sequential filtering techniques to model electronic and media calibration errors in high-precision ranging data, have indicated that substantial improvements in accuracy (factors of 2 to 4) could be **achieved** over the **techniques** previously used in those missions.

This paper describes a new navigation demonstration performed in conjunction with the Galileo spacecraft's second Earth encounter and its subsequent flyby of the asteroid Ida. The demonstration was designed to test an improved sequential filter model, developed as an outgrowth of the demonstrations mentioned above, which may **greatly** improve the accuracy obtainable with two-way Doppler, the data type most often used in **radio** navigation. The principal features of the new filter model, dubbed the "enhanced" filter, are the incorporation of several stochastic models to represent the principal ground system error sources affecting the data, and frequent (hourly) updates of the filter parameter estimates. This filter was originally proposed in a study comparing navigation accuracy statistics obtained with different filtering schemes and different mathematical representations of the Doppler data type [Ref. 3], and has been evaluated with the use of additional data **types** in other studies [Ref. 4].

## THE GALILEO MISSION

The Galileo spacecraft was launched towards Jupiter on October 18, 1989 using a Venus-Earth-Earth Gravity Assist (**VEEGA**) trajectory. On December 8, 1992, the spacecraft flew by the Earth at an altitude of 303 km on the final gravity assist which propelled it to Jupiter. During the Earth-Jupiter cruise phase of the mission, the spacecraft encountered the asteroid Ida on August 28, 1993. For each of these events, **accurate** estimates of the **spacecraft** trajectory were needed to design the targeting **maneuvers**.

Due to the failure of the High Gain Antenna (**HGA**) to deploy, the spacecraft navigation was accomplished using the Low Gain Antenna (**LGA**). The data from the LGA consisted of two-way Doppler, **two-way** range, and ADOR data points acquired at S-band frequencies. Doppler data measures the frequency shift caused by the line-of-sight component of the velocity of the spacecraft with respect to the tracking station. Errors in this data type are caused by delays induced by the medium in which the signal travels, specifically by the ionosphere and troposphere of the Earth. Gross **errors** caused by the media are generally removed by calibrating the data with external information of the media delays, but residual noise still remains. S-band Doppler data in particular is fairly sensitive to ionospheric and tropospheric effects, and thus its noise level (assumed **measurement** uncertainty) is higher than X-band Doppler. For this phase of the mission where the spacecraft was fairly near the Earth, the Doppler data was quite good with the noise always under 1 mm/sec for a 60-second count time. operationally, the Doppler data was nominally weighted at 1-2 mm/s since it was **assumed** that the filter could not properly model the media and Earth orientation errors. In this paper, we show however that those errors can be modeled and explicitly solved for, resulting in an improved solution.

Range data is acquired by measuring the time between **the** transmission and reception of a ranging signal. Range data was consistently available during the Earth encounter phase of the mission with the **point-to-point** noise **level** varying from around 10 m to 20 m. Because station calibration errors and solar plasma effects tend to bias entire range passes by around 5-10 m, the range data is generally **deweighted** in the solution. In our fits, the range was assigned a weight of 100 m.

ADOR data is an **interferometric** data type in which one-way range data from the spacecraft received at two stations is difference with similar signals from a nearby quasar. This differencing effectively removes much of the atmospheric effects and gives a measurement of the angular separation of the spacecraft from the quasar. The ADOR data augments the Doppler and range by providing information in the **directions** perpendicular to the line-of-sight to the spacecraft. The operational **trajectory** solutions which used ADOR data provided one basis for comparison with the results obtained using the enhanced filter model.

## FILTER STRATEGY

Orbit determination accuracy is heavily dependent on the models used to represent the spacecraft's orbit and the error sources affecting the data. The force models used to integrate the trajectory include the gravitational attraction of the sun, moon and the nine planets, solar radiation pressure, and spacecraft **propulsive** events. Error sources affecting the data include path length delays due to the troposphere and ionosphere and errors associated with DSN station locations. Operationally, estimated parameters (**parameters** which **were** adjusted to obtain the best least-squares fit to the data) included the state, solar

radiation **pressure**, the Earth's **ephemeris**, and **three** Cartesian impulsive AV components of **all** propulsive events. **Solar** radiation pressure was **modelled** using a flat plate representation of **the spacecraft**, and the estimated parameters in this model are the specular and diffuse reflectivity coefficients of the flat plate. Propulsive events include Trajectory Correction Maneuvers (**TCMs**), attitude update turns and line flushings of the retro-propulsion module (RPM). Due to **the** wide **beamwidth** of the LGA, the spacecraft did not have to be pointed directly at the Earth at all times, and attitude updates occurred relatively infrequently. Line flushings were used to clear the propellant lines of the buildup of oxidants and occurred at roughly 23 day intervals. The flushings have known magnitudes and directions which were input prior to fitting the data. They generally solved to within 1 mm/s of their a-priori values.

Consider parameters (parameters which contribute to the formal uncertainty of the fit but are not actually adjusted) in the standard filter included the Earth's ephemeris, tropospheric and ionospheric path delays, and station location uncertainties. For the enhanced filter, all these consider parameters were placed in the estimate list. In addition, four other parameters were also **estimated**. These included two components of the **Earth's** polar motion, a term for the variable rotation rate of the Earth, and a term representing the random biases in the Doppler data due to **unmodeled** effects on the data such as solar plasma. Except for the Earth ephemeris and station locations, all **were** modeled as exponentially correlated process noise with zero mean. A batch-sequential **filter** algorithm was used to perform the fit. Table 1 lists **all** these parameters and their a-priori uncertainties. In addition, for the stochastic parameters, the **decorrelation** time is also given. For a more detailed description of these parameters, see reference [31].

Parameter	A-priori Uncertainty (1 sigma)
State (Cartesian position and velocity)	10 <sup>8</sup> km
Specular and diffuse radiation coefficients	10% of nominal solar radiation pressure value
Earth ephemeris <sup>1</sup>	0.2 km, radial, 17 km downtrack, and 30 km normal (in heliocentric coordinates)
TCMS	10% of nominal AV
Attitude update turns	2 mm/s, spherical
RPM's	1 mm/s along axial direction, 0.5 mm/s in the other two components, <b>constrained</b>
<b>Troposphere</b>	40 cm wet, 10 cm dry (2 <b>hr decorrelation</b> time)
Ionosphere	75 cm day, 15 cm night (3 <b>hr decorrelation</b> time)
Station location	50 cm in spin radius, 6 m in z-height, 70 cm in longitude
Polar motion	5x10 <sup>-8</sup> rad (1 day <b>decorrelation</b> time)
Earth rotation	0.65 msc (0.5 day <b>decorrelation</b> time)
Doppler bias	3 <b>mHz (3 day decorrelation</b> time)

<sup>1</sup>The Earth ephemeris in the filter is modeled in terms of Brewer and **Clemence Set III** parameters. For this table, they were transformed to radial, **downtrack**, and normal heliocentric coordinates for a simpler description of their uncertainties.

One **final** note to mention is that the data arc used for the Ma approach had several anomalous propulsive events which also had to be estimated in the filter. One was a test of the spacecraft's capability to use its spin thrusters to spin-up to 10 rpm from its nominal rate of 2.88 rpm, and then back down to the **nominal**. Because this had never been **tried** before, the net AV it would incur was not known beforehand. Thus, it was modeled in the **filter** as a zero AV impulse, with an uncertainty of 20 mm/s. Another anomalous event was an **accidentally** unbalanced sequence of thruster firings used for two RPM flushing events. Because a rough idea of the magnitude and direction of the imbalance was known, nominal values were input for the net AV and its uncertainty.

RESULTS - EARTH-2

In order to test the validity of the models and assumptions, cases were needed for which solutions using the enhanced filter could be compared with solutions that used the standard filter and assumptions. Especially useful were cases where ADOR data was used in the fit, as this data produces a better solution than Doppler and range alone, at the expense of added cost and complexity associated with obtaining the differential measurement. The first of these test cases was provided by solutions used to target the final maneuver for the **Earth-2** encounter, which took place on December 8, 1992. The data arc for this solution started on October 15, 1992, and ended on November 22, 1992. In addition to nearly continuous passes of Doppler and range, 19 ADOR points (9 from the **Goldstone-Madrid**, and 10 from **Goldstone-Canberra** baselines) were used for the operational OD solution. The fit used a data weight of 1 mm/s for Doppler, 100 m for range, and 50 cm for the ADOR data. The result of this fit and its 1-sigma uncertainty ellipse is shown in Figure 1 in the Earth B-plane (for a definition of the B-plane, see Appendix 1). Table 2 lists the corresponding estimate and uncertainty in the Time of Closest Approach (TCA). Also shown in Figure 1 and Table 2 are standard filter solutions and uncertainties without the ADOR data. These can be compared with the "truth" - a post-flyby reconstruction of the trajectory -- which shows with high accuracy where the spacecraft actually went. It can be seen from the figure and table that both solutions using the standard filter were accurate within the limits of their uncertainties, but the ADOR solution is noticeably better in the B-plane, with a miss of only 1.7 km as opposed to 5.6 km.

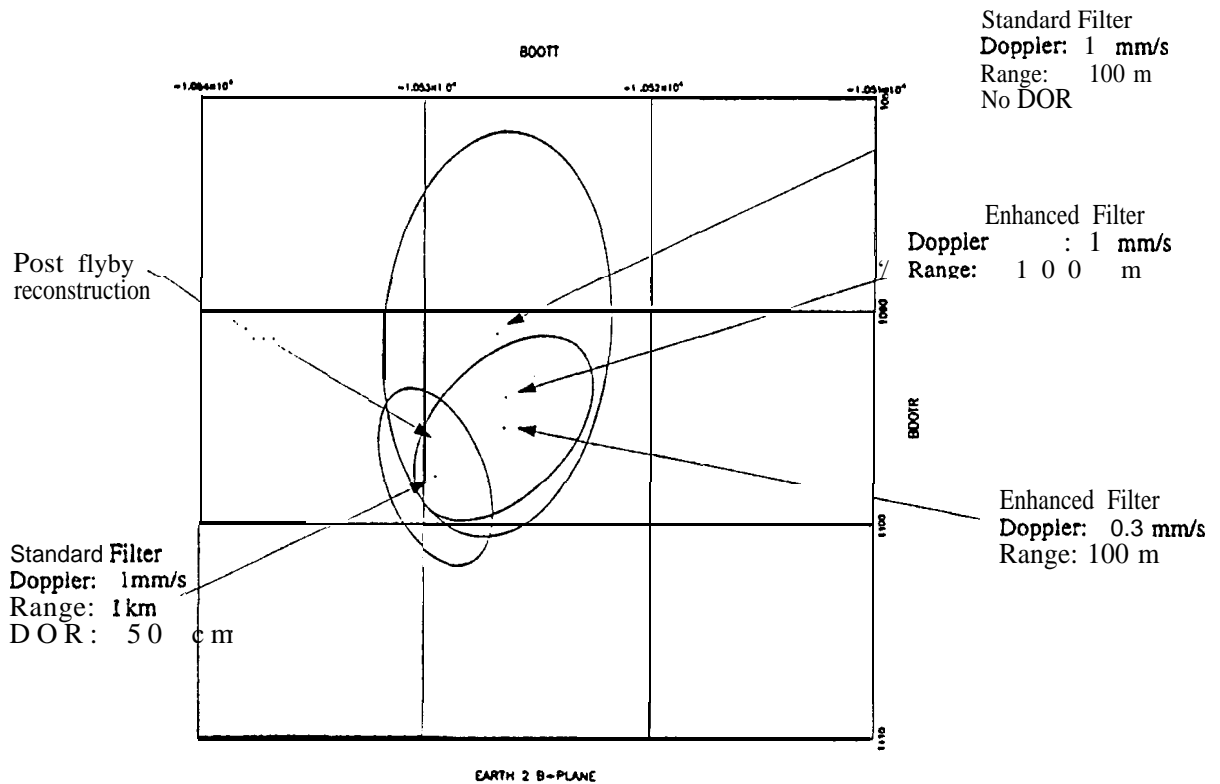


Figure 1: B-plane at Earth-2

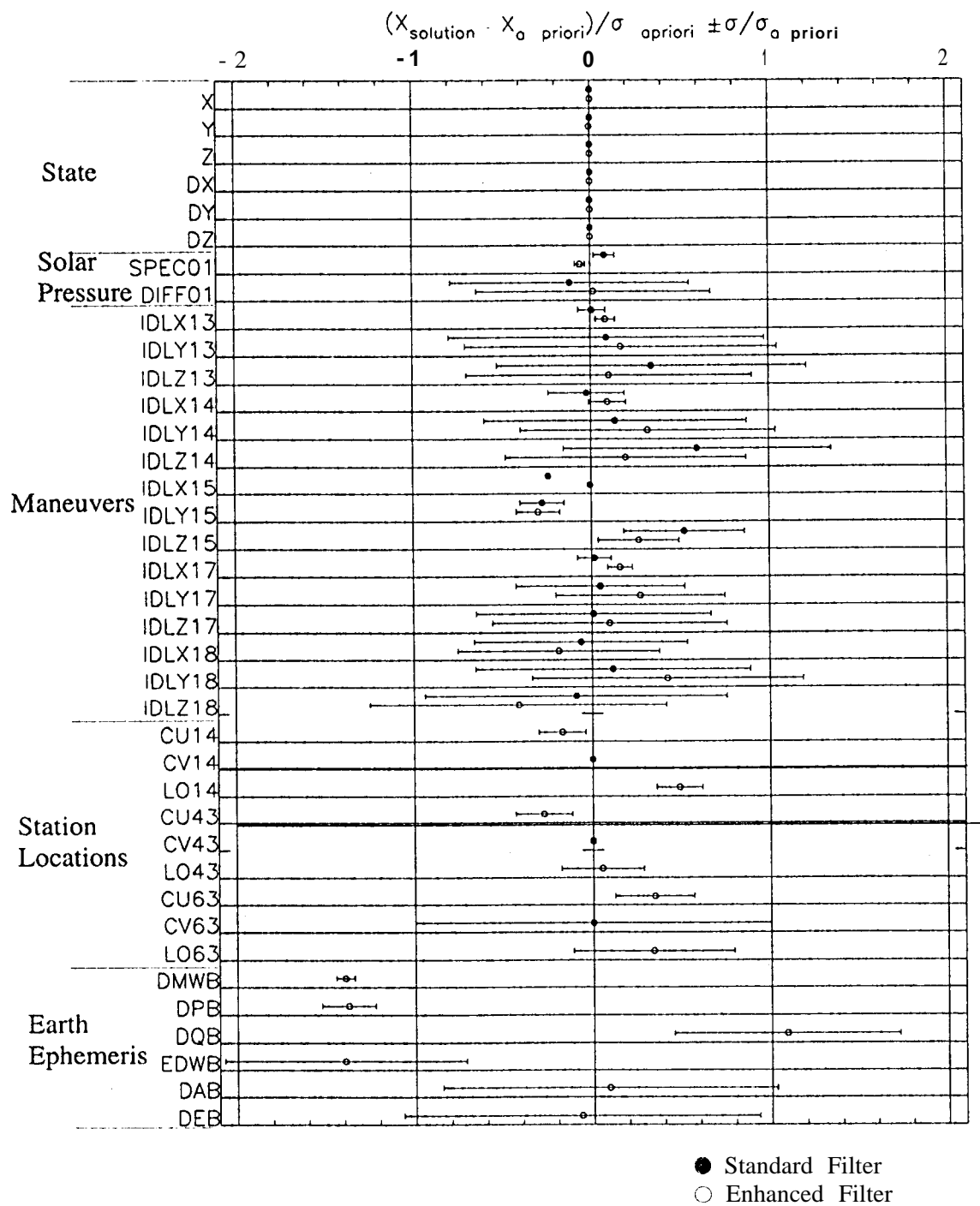
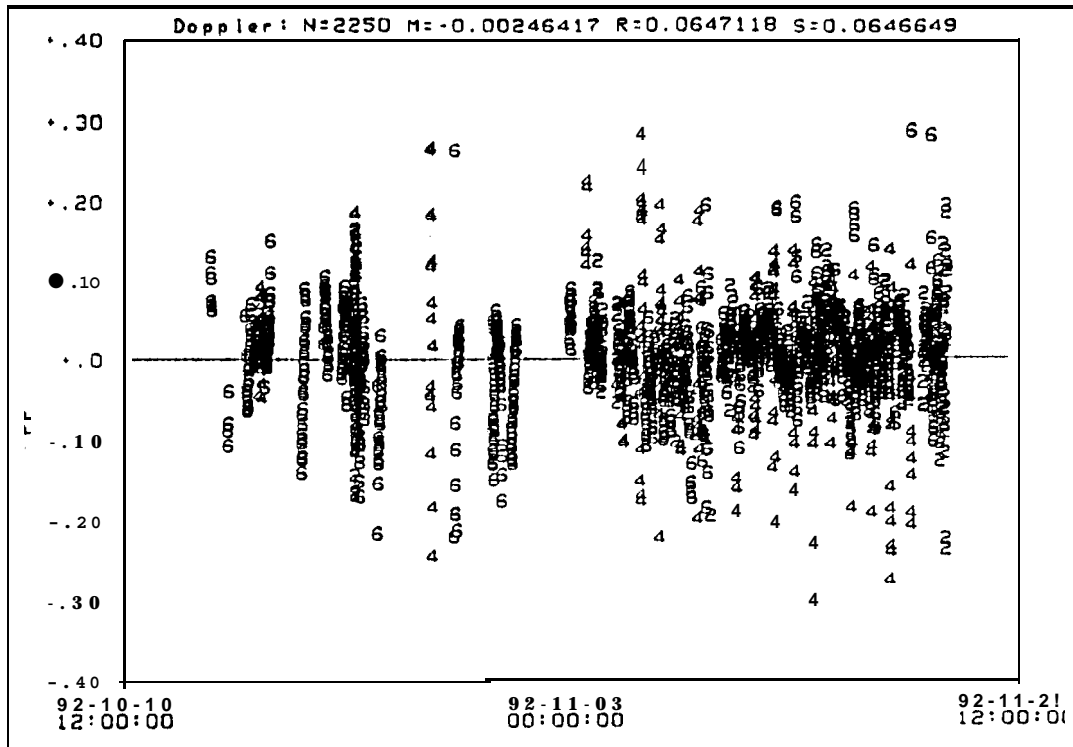


Figure 2: Comparison of Estimated Parameters between the Standard and Enhanced Filters

(a) Standard Filter



(b) Enhanced Filter

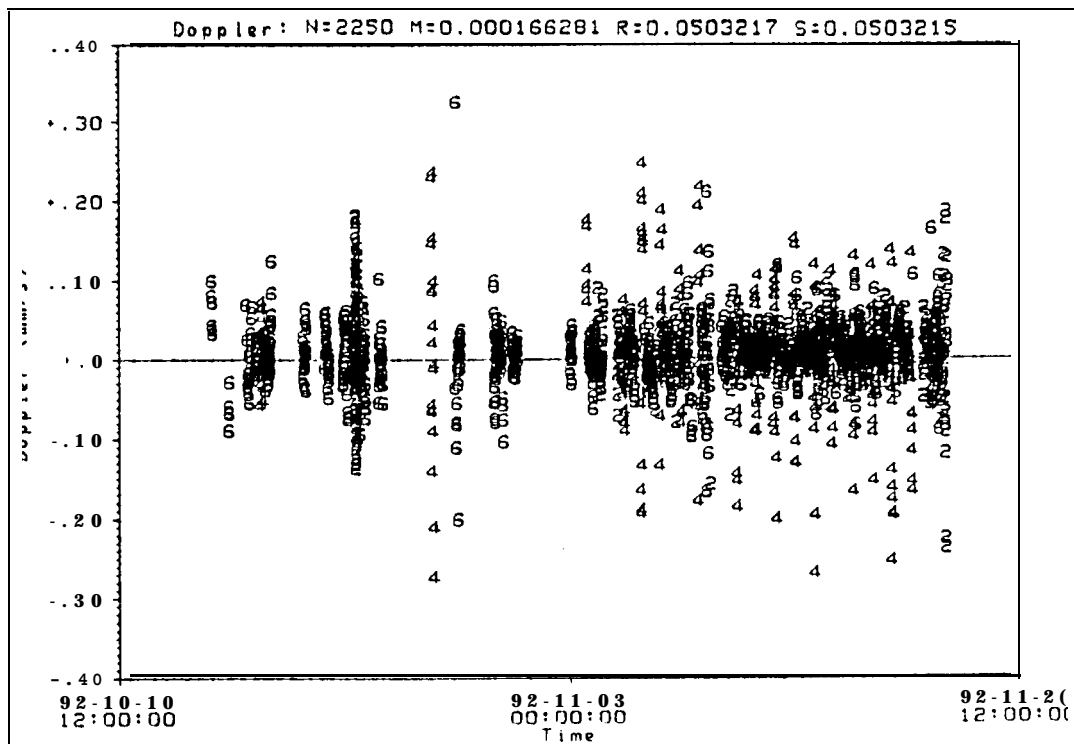


Figure 3: Earth-2 Doppler Residuals for (a) Standard Filter, and (b) Enhanced Filter

The question then remains as to how well the improved filter performs. Two cases are shown, the first with the Doppler weight kept at 1 mm/s, and the second with the weight increased to 0.3 mm/s. The weight for the range data was kept the same as before, 100 m. The B-plane results are also plotted in Figure 1 and the TCA listed in Table 2. Both solutions did quite well in predicting the spacecraft's trajectory, with the B-plane miss of 3.5 and 2.9 km for the 1 mm/s and 0.3 mm/s solutions, respectively. As could be expected, tightening the weight on the Doppler moved the solution closer to the actual flyby point. Both solutions are also better in terms of miss distance and post-fit uncertainties than that obtained using a standard Doppler and range fit, but not quite as good as the ADOR solution. The TCA's are not affected much by any of the weights or filters, as this parameter is determined primarily by the range data and is accurately solved for in all cases.

Table 2 TIME OF CLOSEST APPROACH AT EARTH-2 (ON DECEMBER, 8, 1992)	
Solution	TCA (in UTC)
Actual flyby value	15:10:24.0
Standard filter with ADOR data	15:10:24.0 ± 0.0 sec
Standard filter without ADOR data	15:10:23.9 ± 0.2 scc
Enhanced filter, Doppler at 1 mm/s	15:10:23.9 ± 0.2 sec
Enhanced filter, Doppler at 0.3 mm/s	15:10:23.9 ± 0.2 scc

Although this result provides a necessary condition for verifying that the enhanced filter worked properly, by itself it is not sufficient. It could be that the B-plane result is entirely fortuitous, that is, the trajectory was rotated in some fashion so that the encounter B-plane is correct, but the filter computed unreasonable values for the estimated parameters. Thus, as further validation, the solution parameters estimated by the enhanced filter were compared to those obtained by the standard one. The result is shown in graphical form in Figure 2, where the estimated parameters for both filters are plotted along with their uncertainties. In order to plot all parameters on the same graph, the estimated corrections to the nominal were normalized by dividing it by its a-priori 1-sigma uncertainty, and similarly for its post-fit uncertainty. Figure 2 shows that the solutions for the state, solar pressure, and maneuvers computed by the enhanced filter matched reasonably well (within their respective uncertainties) with the estimates computed by the standard filter. Also noticeable, however, is the fact that the enhanced filter estimates of Lieske's Earth's ephemeris parameters are slightly greater than 1-sigma away from its a-priori values (these parameters are not estimated by the standard filter). When transformed, these values correspond to changes of slightly larger than 1-sigma in the downtrack and normal positions of the Earth. Although somewhat unusual, the change in the B-plane caused by these corrections to the Earth's ephemeris is only 1.3 km. Then, since the estimates for the stochastic parameters do not affect the trajectory, it can be reasonably concluded that the standard and enhanced filter solutions describe very similar trajectories and a correct solution was found by the enhanced filter.

It is also instructive to examine the post-fit residuals of the solutions. Figure 3 plots the post-fit Doppler residuals of the standard and enhanced filter. A qualitative examination of the two plots shows that the residuals of the enhanced filter are flatter with the low frequency variations having been damped out. Quantitative results indicate that the residuals of the enhanced filter have slightly smaller root-mean-square values, around 0.05 as opposed to 0.06 mm/s.

## RESULTS - IDA

The second test case was a solution used for navigating the asteroid Ida flyby. Unlike the Earth-2 encounter case, however, there was no "truth" solution which could be used to determine the absolute accuracy of the different filters. Because optical pictures taken of Ida during the final phases of the approach were the strongest data type in the encounter solutions, the post flyby reconstruction was known accurately only relative to Ma itself. Then, due to uncertainties in Ida's ephemeris, the spacecraft's trajectory in

heliocentric space **could** not be precisely determined. As a consequence, an **assessment** of the performance of the **enhanced** filter for this case **can** only be made **relative** to the **standard** solutions.

**The data arc** for the fits started on February 10, 1993 and ended on April 27, 1993, and the solutions **were** mapped to the Ida B-plane. Although good Doppler coverage was obtained during **this** period, the range data was somewhat sparse and its noise level grew noticeably larger as the **spacecraft** distance **increased**. One ADOR point along the **Goldstone-Canberra** baseline, taken on April 24, was used for the operational solution.

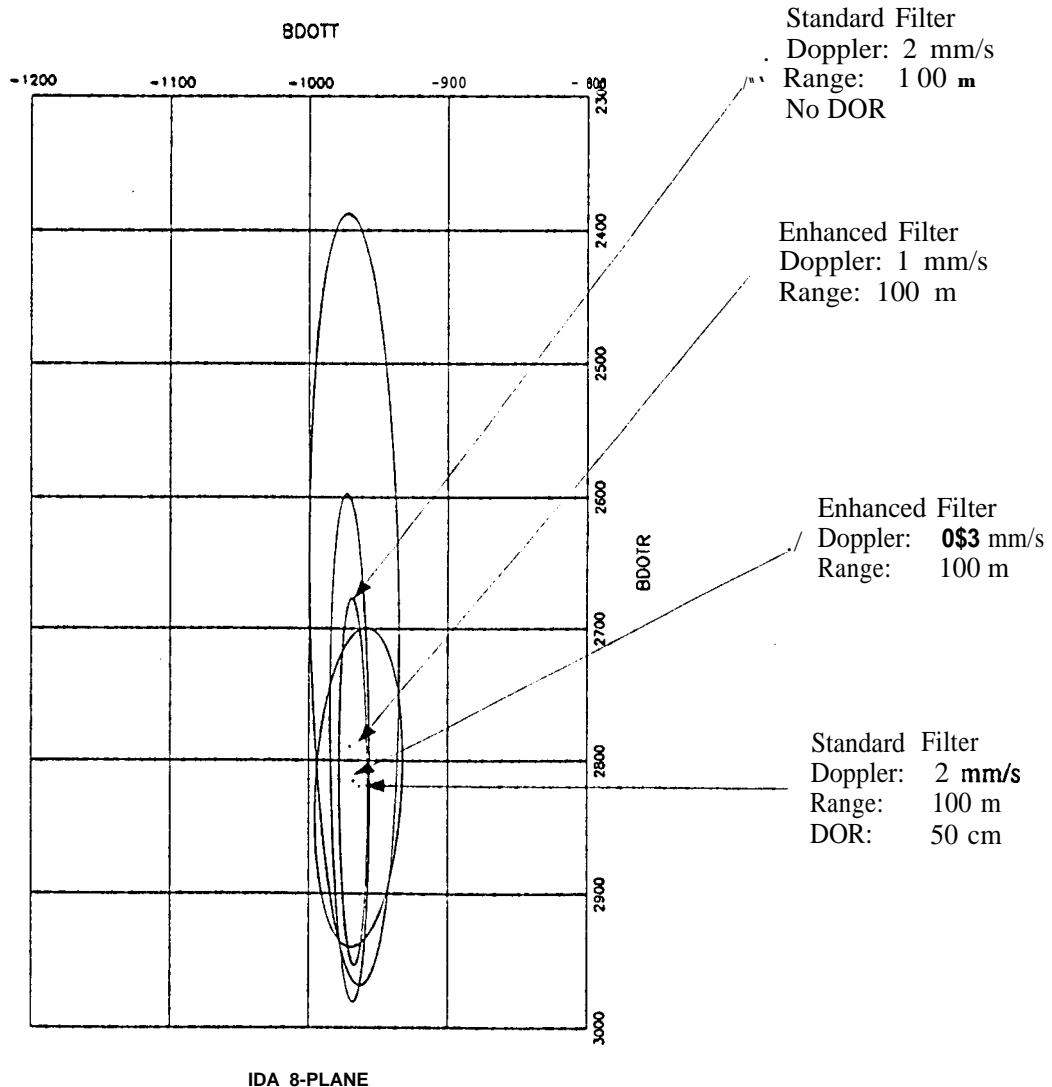


Figure 4: Ida B-plane



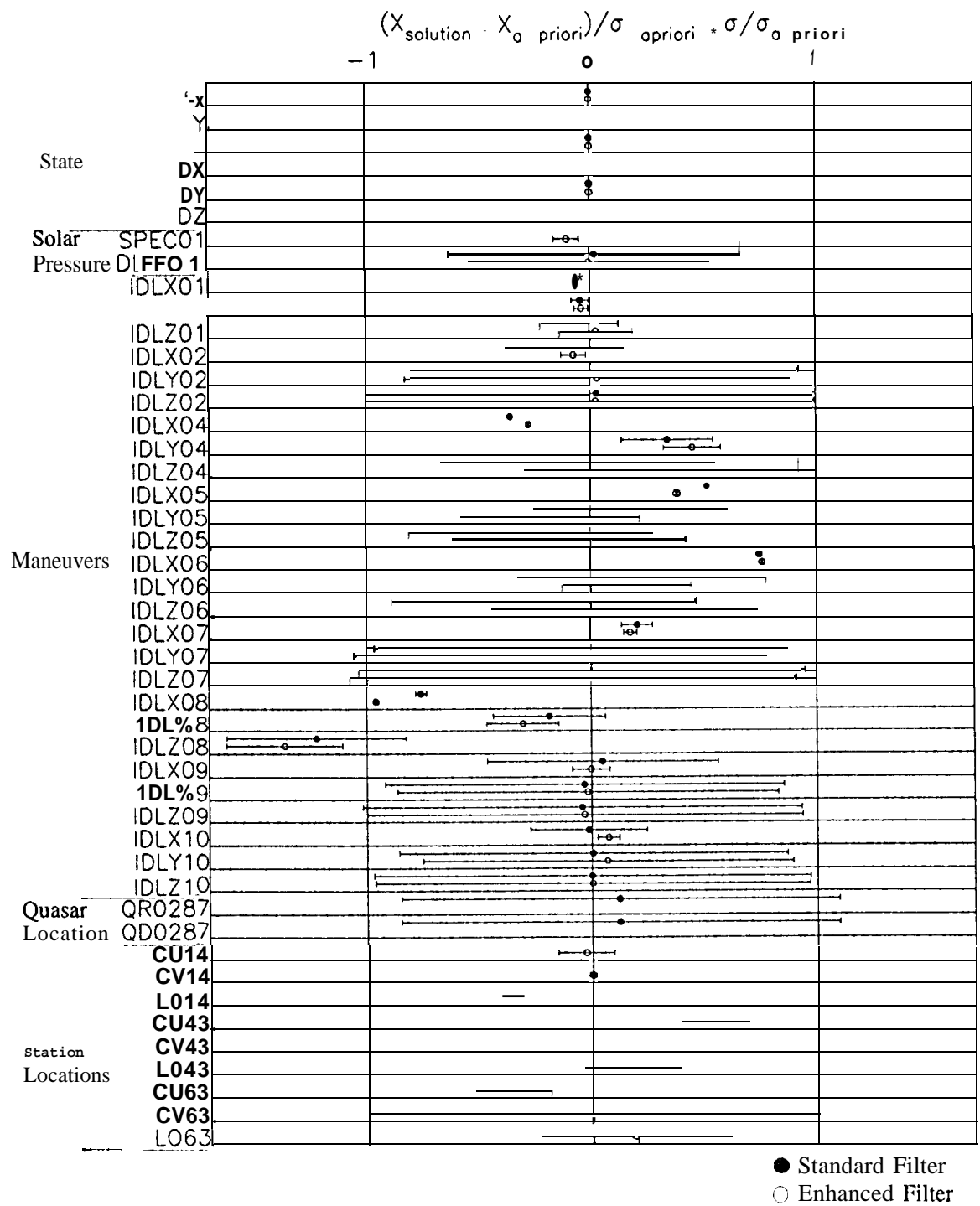


Figure 5: Comparison of Estimated Parameters between Standard and Enhanced Filters for Ida

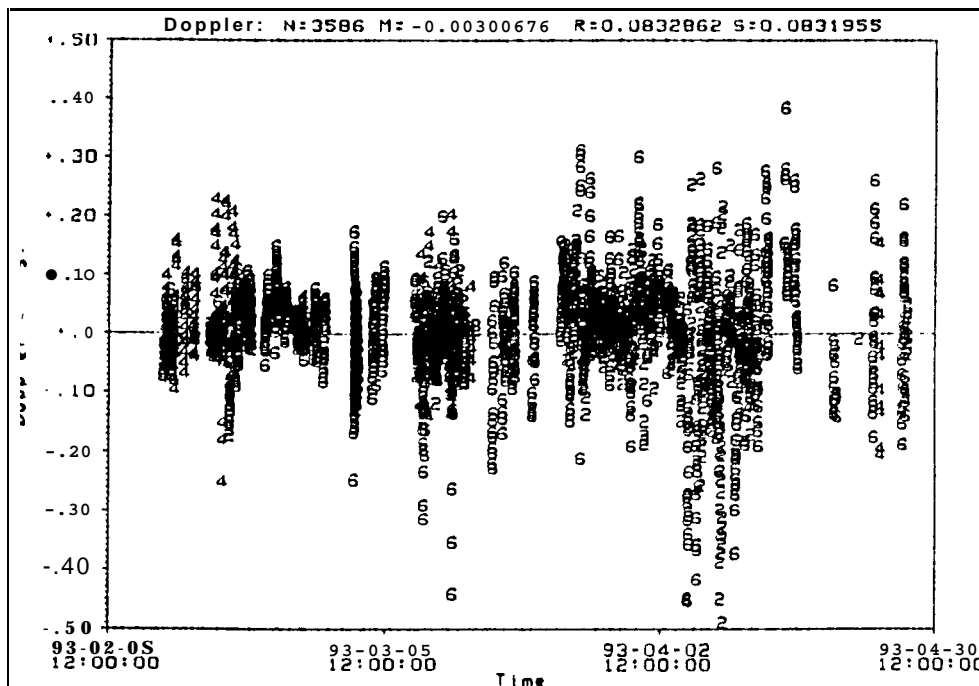
A comparison of four solutions -- two using the standard filter and two using the enhanced filter -- is shown in Figure 4. The two standard solutions use Doppler weighted at 2 mm/s and range weighted at 100 m (except for a **final** range pass, obtained on April 27, which had higher noise and was subsequently weighted at 1 km). One of the standard solutions incorporated the lone available ADOR point, weighted at 1 m. For the two enhanced filter solutions, the Doppler data was weighted at 1.0 and 0.3 mm/s, and the range **data** was weighted the same as for the standard cases. The uncertainty on the radio-only standard solution is quite large, almost 300 km mostly in the **B•R** direction. With the inclusion of the ADOR **point**, this uncertainty is decreased considerably, down to 120 km. Now comparing the two enhanced filter solutions, it can be seen that at **1mm/s**, the solution jumps to about halfway between the radio only and radio plus ADOR value. Increasing the weight further to 0.3 mm/s, the solution is almost identical to the ADOR one. The uncertainty ellipse at 0.3 mm/s is comparable to the ADOR **solution** in **B•R**, and is even better than ADOR in **B•T**. Table 3 lists the associated **TCA's** at Ida. All TCA values are consistent with each other, and the uncertainties for the two **enhanced** filter runs arc at least a factor of two **better** than either of the standard **filter** cases.

Table 3 TIMES OF CLOSEST APPROACH AT IDA (ON AUGUST 28, 1993)	
<b>Solution</b>	<b>TCA (UTC)</b>
Standard filter with ADOR data	16:52:59.7 ± 1.6 sec
Standard filter without ADOR data	16:52:59.3 ± 1.7 sec
Enhanced filter with Doppler at 1.0 mm/s	16:52:59.3 ± 0.8 sec
Enhanced filter with Doppler at 0.3 mm/s	16:52:59.5 ± 0.6 sec

Because the absolute accuracy of the solutions cannot be determined, the solution parameters and data **residuals** for the enhanced filter were examined more closely and compared with the standard filter which used ADOR data. As done for **the** Earth-2 results, the **first** comparison was with the estimated parameters. The normalized estimates and uncertainties for the two filters are shown in Figure 5. Once again, the two solutions are fairly **similar** in all estimated parameters. One unusual point to note is that the estimate for parameter "**IDLZ08**" was greater than its a-prior standard deviation in both cases. This particular parameter is the **z** component of velocity for one of the anomalous thruster flushing events mentioned earlier. **Because** the event was unexpected, a reasonable guess of its maximum magnitude was input as its a-priori uncertainty. However, the event occurred nearly at the end of the data arc, and the filter does not have enough information to properly solve for this parameter. It is interesting, however, that the enhanced filter gave a similar solution as did the ADOR, which is a more direct observation of the **spacecraft's** declination.

A comparison of the Doppler data residuals for this arc is shown in Figure 6. The post-fit rms of the enhanced filter residuals is about 0.05 mm/s, while those of the regular filter were 0.08 mm/s. A visual comparison of the two plots **seems** to indicate that the enhanced filter has flattened out the low-frequency signals, and biases in some of the passes have clearly been removed. For example, a bias of just under 0.1 mm/s in the third from the last pass from the Madrid station evident in the residuals from the regular filter has been removed by the enhanced filter. Another view of the Doppler residuals is shown in Figure 7. Here, a histogram of the **residuals** is plotted for the standard and enhanced filter solutions. If all systematic errors have been removed, then the data would resemble a perfect Gaussian curve. The histogram for the enhanced filter in Figure 7 follows fairly closely to the ideal Gaussian curve. The histogram for the standard filter also is fairly Gaussian in shape, but there are more variations from the curve in the outlying bins which indicate **modelling** or data errors which have not been removed. In addition, **the** tails of **the** distributions dampen out faster in the enhanced filter case, indicating fewer **outlier** points.

(a) Standard Filter



(b) Enhanced Filter

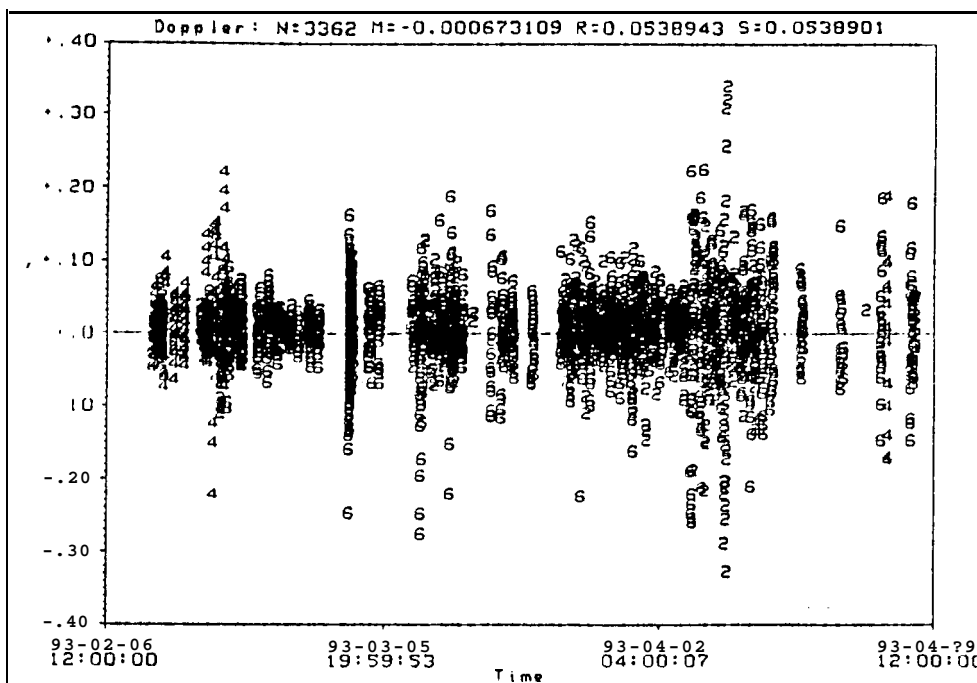


Figure 6: Ida Doppler Residuals for (a) Standard and (b) Enhanced Filter

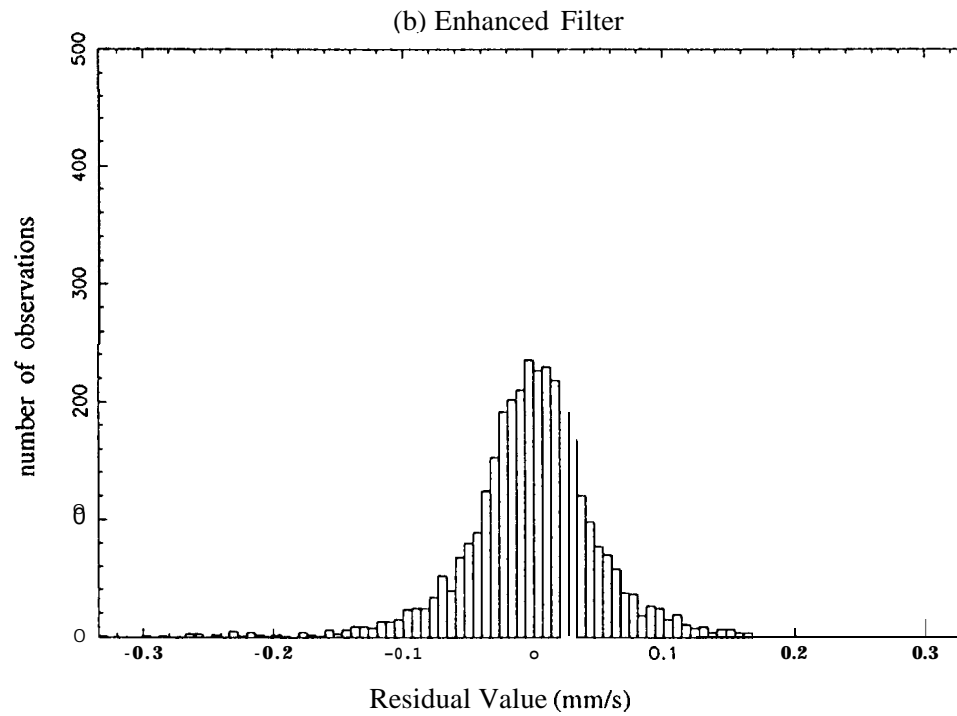
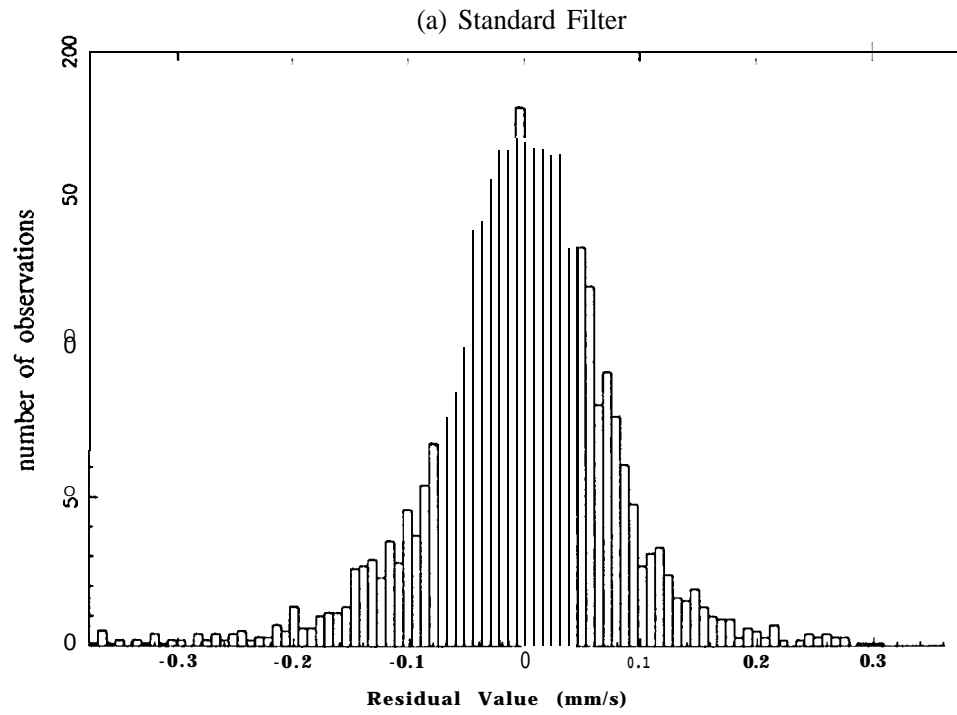


Figure 7: Histogram of Doppler Residuals for (a) Standard and (b) Enhanced Filter

## CONCLUSIONS

In this paper a new sequential filtering scheme for processing radio tracking data, dubbed the "enhanced" filter, was successfully demonstrated with flight data acquired from the Galileo spacecraft. Estimates of the spacecraft trajectory were obtained using this **filter to reduce** tracking data acquired during the approach phases of the Earth-2 and asteroid Ma encounters, respectively. In the case of the Earth-2 encounter, the orbit solution obtained with the enhanced **filter** from Doppler and ranging data yielded about a factor of 2 reduction in both the actual orbit determination error (compared with an accurate post-encounter reconstruction) and the statistical dispersions, relative to a similar solution obtained with the standard operational filter. In the analysis of the Ida pre-encounter tracking data, the estimates of the encounter aim point derived from Doppler and ranging data with the enhanced filter and the operational filter were statistically **consistent**; the statistical uncertainties in the enhanced filter solution were again about a factor of 2 smaller than those of the operational filter. In both the Earth-2 and Ma encounter cases, the enhanced filter Doppler and ranging orbit solutions were found to be in good agreement with the best operational filter solutions, in which ADOR data were used in addition to Doppler and ranging. The statistical dispersions of the enhanced filter were comparable to the ADOR solution in the Earth-2 case, and slightly better in some directions in the Ida case.

## ACKNOWLEDGMENTS

The work described in this paper was carried out at the Jet Propulsion Laboratory, California Institute of Technology, under a contract with the National Aeronautics and Space Administration.

## REFERENCES

1. T. P. **McElrath**, B. Tucker, K. E. **Criddle**, P. R. Menon, and E. S. **Higa**, "Ulysses Navigation at Jupiter Encounter," paper **AIAA-92-4524**, **AIAA/AAS Astrodynamics** Conference, Hilton Head, South Carolina, 10-12 August 1992.
2. V. M. **Pollmeier**, P. H. **Kallemeyn**, and S. W. Thurman, "Application of High-Precision Two-Way S-band Ranging to the Navigation of the Galileo Earth Encounters," paper AAS 93-251, **AAS/GSFC International Symposium on Space Flight Dynamics**, **Greenbelt**, Maryland, 26-30 April 1993,
3. S. W. Thurman and J. A. **Estefan**, "Radio Doppler Navigation of Interplanetary Spacecraft Using Different Data Processing Modes," paper AAS 93-163, **AAS/AIAA Space flight Mechanics Meeting**, Pasadena, **California**, 22-24 **February** 1993.
4. J. A. **Estefan**, V. M. **Pollmeier**, and S. W. Thurman, "Precision X-band Doppler and Ranging Navigation for Current and Future Mars Exploration Missions," paper AAS 93-250, **AAS/GSFC International Symposium on Space Flight Dynamics**, **Greenbelt**, Maryland, 26-30 April 1993.

## APPENDIX

Planetary approach trajectories are typically described in aiming plane coordinates, often referred to as "B-plane" coordinates (see Fig. A-1). The coordinate system is defined by three orthogonal unit vectors,  $\mathbf{I}$ ,  $\mathbf{T}$ , and  $\mathbf{R}$  with the system origin taken to be the center of the target planet. The  $\mathbf{S}$  vector is parallel to the spacecraft velocity vector relative to the target planet at the time of entry into the target planet's gravitational sphere of influence, while  $\mathbf{T}$  is normally specified to lie in the ecliptic plane (the mean plane of the Earth's orbit), however, in this analysis,  $\mathbf{T}$  was defined to lie in the Martian equatorial plane. Finally,  $\mathbf{R}$  completes an orthogonal triad with  $\mathbf{S}$  and  $\mathbf{T}$ .

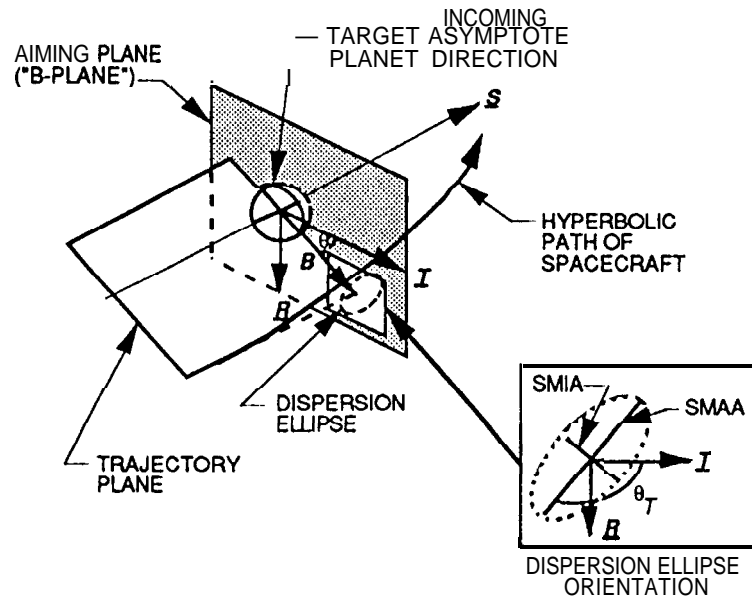


Fig. A-1 Aiming Plane Coordinate System Definition

The aim point for a planetary encounter is defined by the miss vector,  $\mathbf{B}$ , which lies in the  $\mathbf{T}$ - $\mathbf{R}$  plane, and specifies where the point of closest approach would be if the target planet had no mass and did not deflect the flight path. The time from encounter (point of closest approach) is defined by the *linearized time-of-flight (LTOF)*, which specifies what the time of flight to encounter would be if the magnitude of the miss vector were zero. Orbit determination errors are characterized by a one-sigma or three-sigma **B-plane** dispersion ellipse, also shown in Fig. A-1, and the one-sigma or three-sigma uncertainty in LTOF. In Fig. A-1, SMIA and SMAA denote the semi-minor and semi-major axes of the dispersion ellipse, respectively.